

Fission before K equilibration

Zuhua Liu, Huanqiao Zhang, Jincheng Xu, Yu Qiao, Xing Qian,* and Chengjian Lin
China Institute of Atomic Energy, Beijing 102413, China
 (Received 24 April 1995)

It is demonstrated experimentally that the reaction systems on the different side of Businaro-Gallone critical mass asymmetry (α_{BG}) have different characteristics in fusion-fission reactions. Fragment anisotropies resulting from the reactions with the entrance-channel mass asymmetry $\alpha > \alpha_{BG}$ are well described by the saddle-point transition-state model. However, the measured fragment anisotropies for the systems with $\alpha < \alpha_{BG}$ are obviously greater than the predictions of this model at subbarrier and near-barrier energies and gradually tend to coincide with the theoretical expectations as the bombarding energy increasing over fusion barrier. These observations have led us to a suggestion of preequilibrium fission for low angular momentum. The predictions of such a preequilibrium fission model are compared with the available experimental data and it is shown that they can satisfactorily reproduce the observed trends as a function of the bombarding energy for the reaction systems studied. [S0556-2813(96)00507-9]

PACS number(s): 25.70.Jj

I. INTRODUCTION

It is well known that the saddle-point transition-state (SPTS) model has become the standard theory of fission-fragment angular distributions and received great success since it was proposed. However, in a number of fusion-fission reactions with projectiles heavier than $A_p=24$ [1], the fission fragment angular distributions are much more anisotropic than predicted by the SPTS model. It has been suggested [2] that this deviation from the standard theory is an indication of the failure for the compound-nucleus formation in the reaction. The suggested reaction mechanisms include fast fission [3] and quasifission [4] which result in a fission-like fragment without going through a well-defined fission saddle point. Recently, the anomalous anisotropies [5,6] have been observed in the angular distributions induced by the reactions with projectiles lighter than $A_p=20$ at near- and subbarrier energies. To our knowledge, fast fission cannot take place in the low energy cases, because the involved angular momenta are not high enough to make the fission barrier vanished. Very recently, Hinde *et al.* [7] have measured the fission fragment angular distributions for the reaction of $^{16}\text{O}+^{238}\text{U}$ at energies around the Coulomb barrier, and found that the fragment anisotropies rise rapidly, then ultimately seem to saturate, as the bombarding energy decreases through the barrier region. They interpreted this observation as collisions with the tips of the target nuclei resulting in quasifission. As an alternative suggestion for the origin of the observed anomaly, Liu *et al.* [8] have put forward a new version of the preequilibrium fission model. In this paper, we will show further experimental evidence for the assumption of preequilibrium fission.

As pointed out by Ramamurthy and Kapoor [9], characterized evidence for preequilibrium fission would be an entrance-channel dependence of the fragment anisotropies for target-projectile combination across the Businaro-

Gallone (BG) ridge in mass degree of freedom. Ramamurthy *et al.* [10] recently carried out the measurements of the fragment angular distributions for the reactions induced by projectiles lighter than $A_p=20$ on the thorium and neptunium targets at above-barrier energies. Their results show an entrance-channel dependence of the fragment anisotropies. However, in their measurements, the observed fission events included both fusion-fission (FF) and transfer-induced fission (TF) components, making the observed dependence somewhat uncertain. In terms of the fragment folding angle technique, we have separated the FF and TF events, and measured the fragment angular distributions of the FF component for several systems with projectiles lighter than $A_p=20$ at near- and subbarrier energies. Among the measured reaction systems, we have specially chosen $^{11}\text{B}+^{237}\text{Np}$ and $^{16}\text{O}+^{232}\text{Th}$ which both populate the fissioning nucleus ^{248}Cf at the same excitation energies, but on a different side of the BG critical mass asymmetry point. In a letter [8], we have compared the fragment anisotropies as a function of excitation energy for the systems of $^{11}\text{B}+^{237}\text{Np}$ and $^{16}\text{O}+^{232}\text{Th}$, and found that there exist distinguishable differences in the experimental data between these systems. From the above statements, it may be seen that our results would give more reliable evidence for the entrance-channel dependence of the fragment anisotropies. Besides, we found that the near- and subbarrier data could provide much clearer evidence of this entrance-channel dependence than the above-barrier data. Actually, at well-above-barrier energies, the experimental fragment anisotropies from the reactions with projectiles lighter than $A_p=20$ are in agreement with the predictions of the SPTS model in which it is assumed that fission is independent of its formation history.

In this paper, we will show our main experimental results and demonstrate experimentally that the reaction systems on a different side of the Businaro-Gallone critical mass asymmetry have different characteristics in subbarrier fusion-fission reactions. Such a characterized behavior in fusion-fission reactions with respect to the entrance-channel mass asymmetry provides further experimental verification of the preequilibrium fission assumption. So far, the puzzling prob-

*Present address: Department of Technical Physics, Peking University.

lem of the anomalous fragment anisotropies observed in the subbarrier fusion-fission reactions can be understood on the basis of our preequilibrium fission model.

II. EXPERIMENTAL PROCEDURE

The experiments were performed using the collimated ^{11}B , ^{12}C beams from the HI-13 tandem accelerator at the China Institute of Atomic Energy, Beijing. The ^{238}U and ^{237}Np targets were about $350 \mu\text{g}/\text{cm}^2$ thick. A Si(Au) detector was placed at -20° relative to the beam direction as a monitor to detect the elastic scattering. Fission fragments were detected by two X - Y position sensitive double-grid avalanche counters (DGAC's) with an active area of $25 \times 20 \text{ cm}^2$, which were placed at either side of the beam. In terms of the difference of the fragment folding angle distributions, we have successfully separated the fusion-fission and transfer-induced fission events, and measured the FF angular distributions for the $^{11}\text{B} + ^{238}\text{U}$, $^{11}\text{B} + ^{237}\text{Np}$, and $^{12}\text{C} + ^{237}\text{Np}$ systems at near- and subbarrier energies. In the process of data treatments, a cut of a horizontal slice of 4 cm was made in the center region of the forward DGAC detector, and the condition $(\theta_{F1})_{\text{c.m.}} + (\theta_{F2})_{\text{c.m.}} = 180^\circ \pm 2^\circ$ for each event was required. Here, $(\theta_{F1})_{\text{c.m.}}$ and $(\theta_{F2})_{\text{c.m.}}$ are the emitting angles of the detected particles in the center-of-mass system. The angular range was set wide enough so that all of the fusion-fission events were within this window. The experimental details were described elsewhere [11]. We find that it is very important to set rather strict conditions to rule out the events of the accidental coincidence between the projectilelike particle and fission fragment, because the DGAC detectors are sensitive to projectilelike particles. In the previous treatment of our data [12], we had not imposed this condition, so that these accidental coincidences were not completely ruled out. Therefore, the data published in [12] are wrong and the relevant conclusions are not correct. In order to correct the mistakes, we have reanalyzed the experimental data for the $^{11}\text{B} + ^{238}\text{U}$ and $^{12}\text{C} + ^{237}\text{Th}$ systems.

III. EXPERIMENTAL RESULTS

The measured FF angular distributions were extrapolated to 0° in terms of the Legendre polynomial with even terms, and the corresponding fragment anisotropies, A_{expt} were calculated. The absolute fusion-fission cross sections were obtained by integrating the Legendre polynomial fit of the angular distributions and normalizing them to the Rutherford scattering cross sections. The experimental errors include the counting statistics, the correction uncertainty of the fragment folding angle distribution overlap and error of the extrapolation of the angular distribution, etc. The total uncertainties for the fragment anisotropies range between 5% and 8%, while for the fission cross sections between 8% and 15%. For the reactions of $^{11}\text{B} + ^{238}\text{U}$, $^{11}\text{B} + ^{237}\text{Np}$, and $^{12}\text{C} + ^{237}\text{Np}$, the detected transfer-fission events are in the range 0.15–2 % of the total fission events. Within the experimental error, the fragment anisotropies before and after correction of the TF component are the same for the B and C induced fission reactions. Our experimental data are summarized in Table I.

A. Fission excitation function

The theoretical fusion excitation functions were calculated in terms of the coupled-channels model [13]. In these coupled-channel calculations, the effects of the target static deformations ($\beta_2=0.224$, $\beta_4=0.050$ for ^{238}U and $\beta_2=0.26$ for ^{237}Np) were taken into account. The inelastic channels, the 0.7319 MeV state of ^{238}U with $\beta_3=0.084$ and the 0.0759 MeV state of ^{237}Np with $\beta_2=0.19$, were coupled to the entrance elastic channel in the calculations, respectively. Displayed in Fig. 1 are the excitation functions for the reaction systems of $^{11}\text{B} + ^{238}\text{U}$, $^{11}\text{B} + ^{237}\text{Np}$, and $^{12}\text{C} + ^{237}\text{Np}$. The solid lines in the figure are the results of the coupled-channel calculations. It may be seen from Fig. 1 that the agreement between the experimental and theoretical excitation functions is quite satisfactory for all three systems. The angular momentum distributions $\sigma_F(J)$ and their second moment $\langle J^2 \rangle_{\text{theory}}$ values were extracted from these calculations.

B. Entrance-channel dependence of fragment anisotropies

Displayed in Fig. 2 is the ratio, $A_{\text{expt}}/A_{\text{theory}}$ versus $E_{\text{c.m.}}/V_B$. Here $E_{\text{c.m.}}$ is the center-of-mass energy, V_B is the height of fusion barrier, and A_{theory} the theoretical fragment anisotropy of the SPTS model. In the treatment of the SPTS model, the K distribution is Gaussian with the variance

$$K_0^2 = \mathcal{G}_{\text{eff}} T_{\text{sad.}} / \hbar^2. \quad (1)$$

Here, the effective moment of inertia \mathcal{G}_{eff} is equal to $\mathcal{G}_{\parallel}\mathcal{G}_{\perp}/(\mathcal{G}_{\perp}-\mathcal{G}_{\parallel})$. \mathcal{G}_{\parallel} and \mathcal{G}_{\perp} are the moments of inertia rotating around the symmetric and perpendicular axes of the nucleus at saddle point, respectively. They were calculated in terms of the rotating finite-range model (RFRM) [14]. $T_{\text{sad.}}$ is the nuclear temperature at saddle point,

$$T_{\text{sad.}} = \left[\frac{E_{\text{c.m.}} + Q - B_f(J) - E_n}{A_{CN}/8} \right]^{1/2}, \quad (2)$$

where Q and $B_f(J)$ are the reaction Q value and fission barrier height of RFRM, respectively. A_{CN} is the mass number of the composite system. E_n is the energy carried away by prefission neutron emission [15,16]. In the calculations of the SPTS model, the angular momentum distributions $\sigma_F(J)$ were taken from the coupled-channels model [13] fit of the measured fusion-fission cross sections. In the figure, α is the entrance-channel mass asymmetry defined as $\alpha = (A_T - A_P)/(A_T + A_P)$. The BG critical mass asymmetry, α_{BG} is about 0.9 for the range of nuclei studied. In order to make a comparison, we also displayed in Fig. 2 the results [11,17] of the reaction systems $^{16}\text{O} + ^{232}\text{Th}$, $^{19}\text{F} + ^{232}\text{Th}$, and $^{16}\text{O} + ^{238}\text{U}$. Some trends in the experimental data are immediately obvious and worth noting. First, the systems on the different side of α_{BG} show different characters in fusion-fission reactions. For the reaction systems with $\alpha > \alpha_{\text{BG}}$, the measured fragment anisotropies are in general agreement with the predictions of the SPTS model. On the other hand, for the systems with $\alpha < \alpha_{\text{BG}}$, the measured fragment anisotropies are obviously greater than expected on the basis of the SPTS model. Second, in the latter case, the differences between the experimental and theoretical values depend on

TABLE I. The experimental results. X and α are the fissility parameter and entrance-channel mass asymmetry, respectively.

| System | Compound nucleus | X | α | $E_{c.m.}$ (MeV) | σ_F (mb) | A_{expt} | $\langle J^2 \rangle_{\text{expt}}^a$ | $\langle J^2 \rangle_{\text{expt}}^b$ | | | | |
|-----------------------------------|-------------------|-------------------|---------------|-----------------------------------|--------------------|-------------------|---------------------------------------|---------------------------------------|----------------|-------------------|--------------|--|
| $^{11}\text{B} + ^{238}\text{U}$ | ^{249}Bk | 0.8134 | 0.9116 | 46.53 | 2.4 ± 0.5 | 1.122 ± 0.074 | 80 ± 49 | | | | | |
| | | | | 47.49 | 7.2 ± 1.5 | 1.133 ± 0.066 | 89 ± 44 | | | | | |
| | | | | 48.47 | 25.5 ± 5.0 | 1.151 ± 0.066 | 101 ± 44 | | | | | |
| | | | | 49.45 | 42.7 ± 8.0 | 1.152 ± 0.076 | 103 ± 52 | | | | | |
| | | | | 50.41 | 99 ± 20 | 1.220 ± 0.070 | 150 ± 48 | | | | | |
| | | | | 51.39 | 147 ± 30 | 1.255 ± 0.067 | 176 ± 46 | | | | | |
| | | | | 52.35 | 231 ± 46 | 1.253 ± 0.057 | 176 ± 40 | | | | | |
| | | | | 53.33 | 272 ± 50 | 1.286 ± 0.073 | 200 ± 51 | | | | | |
| | | | | 54.29 | 350 ± 70 | 1.323 ± 0.077 | 228 ± 54 | | | | | |
| | | | | 56.23 | 451 ± 90 | 1.402 ± 0.082 | 287 ± 59 | | | | | |
| | | | | $^{11}\text{B} + ^{237}\text{Np}$ | ^{248}Cf | 0.8258 | 0.9113 | 49.88 | 3.4 ± 0.8 | 1.133 ± 0.092 | 98 ± 68 | |
| | | | | | | | | 51.66 | 15.3 ± 3.2 | 1.114 ± 0.070 | 86 ± 53 | |
| | | | | | | | | 52.60 | 30.4 ± 6.1 | 1.181 ± 0.079 | 137 ± 60 | |
| | | | | | | | | 53.53 | 53 ± 10 | 1.151 ± 0.069 | 115 ± 53 | |
| 55.41 | 115 ± 21 | 1.297 ± 0.075 | 230 ± 58 | | | | | | | | | |
| 57.28 | 167 ± 34 | 1.335 ± 0.077 | 263 ± 61 | | | | | | | | | |
| $^{16}\text{O} + ^{232}\text{Th}$ | ^{248}Cf | 0.8258 | 0.8710 | 61.16 | 501 ± 95 | 1.358 ± 0.077 | 290 ± 62 | | | | | |
| | | | | 68.81 | 925 ± 167 | 1.621 ± 0.081 | 533 ± 69 | | | | | |
| | | | | 72.61 | 0.33 ± 0.07 | 1.535 ± 0.091 | 389 ± 66 | 82 ± 14 | | | | |
| | | | | 74.49 | 2.0 ± 0.3 | 1.684 ± 0.067 | 505 ± 49 | 127 ± 13 | | | | |
| | | | | 75.43 | 3.6 ± 0.5 | 1.715 ± 0.067 | 531 ± 50 | 157 ± 16 | | | | |
| | | | | 76.36 | 7.1 ± 0.7 | 1.785 ± 0.074 | 588 ± 55 | 197 ± 20 | | | | |
| $^{19}\text{F} + ^{232}\text{Th}$ | ^{251}Es | 0.8337 | 0.8486 | 78.24 | 16.2 ± 1.4 | 1.738 ± 0.083 | 560 ± 63 | 231 ± 26 | | | | |
| | | | | 80.11 | 34.8 ± 2.2 | 1.701 ± 0.056 | 539 ± 30 | 253 ± 19 | | | | |
| | | | | 78.00 | 0.36 ± 0.08 | | | | | | | |
| | | | | 80.80 | 2.21 ± 0.42 | 1.913 ± 0.081 | 741 ± 66 | 222 ± 22 | | | | |
| | | | | 82.70 | 6.49 ± 0.95 | 2.145 ± 0.080 | 945 ± 66 | 363 ± 27 | | | | |
| | | | | 84.50 | 15.2 ± 1.9 | 2.231 ± 0.078 | 1030 ± 65 | 443 ± 31 | | | | |
| $^{12}\text{C} + ^{237}\text{Np}$ | ^{249}Es | 0.8361 | 0.9036 | 87.40 | 44.6 ± 4.6 | 1.988 ± 0.065 | 846 ± 56 | 431 ± 30 | | | | |
| | | | | 92.00 | 169 ± 14 | 1.795 ± 0.063 | 705 ± 60 | 445 ± 34 | | | | |
| | | | | 96.80 | 349 ± 20 | 1.953 ± 0.058 | 877 ± 53 | 606 ± 37 | | | | |
| | | | | 56.90 | 0.34 ± 0.10 | | | | | | | |
| | | | | 57.90 | 1.35 ± 0.36 | | | | | | | |
| | | | | 58.86 | 4.5 ± 1.0 | 1.089 ± 0.092 | 68 ± 70 | | | | | |
| | | | | 60.72 | 17.3 ± 3.6 | | | | | | | |
| | | | | 61.72 | 25.8 ± 4.8 | 1.105 ± 0.070 | 82 ± 55 | | | | | |
| | | | | 62.68 | 45.5 ± 8.4 | 1.135 ± 0.070 | 107 ± 55 | | | | | |
| | | | | 63.60 | 80 ± 15 | 1.176 ± 0.056 | 141 ± 45 | | | | | |
| $^{16}\text{O} + ^{238}\text{U}$ | ^{254}Fm | 0.8415 | 0.8740 | 64.58 | 103 ± 17 | 1.253 ± 0.054 | 204 ± 44 | | | | | |
| | | | | 66.48 | 174 ± 34 | 1.280 ± 0.059 | 228 ± 48 | | | | | |
| | | | | 71.24 | 407 ± 58 | 1.370 ± 0.059 | 318 ± 51 | | | | | |
| | | | | 76.01 | 617 ± 76 | 1.523 ± 0.059 | 471 ± 53 | | | | | |
| | | | | 76.49 | 5.5 ± 0.9 | 1.771 ± 0.080 | 639 ± 66 | 155 ± 16 | | | | |
| | | | | 78.36 | 17.6 ± 1.7 | 1.684 ± 0.058 | 577 ± 49 | 190 ± 16 | | | | |
| 80.24 | 35.9 ± 2.7 | 1.653 ± 0.057 | 561 ± 49 | 227 ± 20 | | | | | | | | |
| 84.09 | 122 ± 7 | 1.650 ± 0.138 | 595 ± 126 | 278 ± 31 | | | | | | | | |

^aThe data of $\langle J^2 \rangle_{\text{expt}}$ were extracted in terms of the K_0^2 values.

^bThe data of $\langle J^2 \rangle_{\text{expt}}$ were extracted in terms of the $\langle \sigma_K^2(J) \rangle$ values.

bombarding energy. At subbarrier and near-barrier energies, the experimental data deviate from the theoretical calculations. As bombarding energy increasing over V_B , the measured anisotropies gradually tend to coincide with the expectations of the SPTS model, which is consistent with Back's observations [18].

C. The mean-square angular momentum

It is well established that the anisotropy of the fission-fragment angular distribution can be characterized by the approximate relation

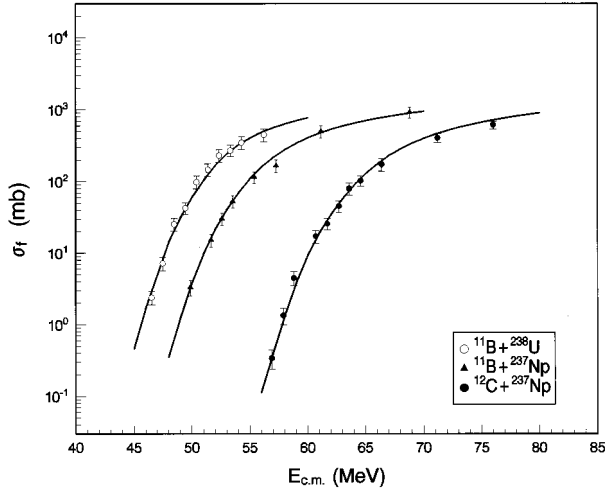


FIG. 1. Fission excitation functions. The solid curves are the results of the coupled-channels calculations.

$$A = 1 + \frac{\langle J^2 \rangle}{4K_0^2}. \quad (3)$$

If the values of K_0^2 is known, then the mean-square angular momentum $\langle J^2 \rangle_{\text{expt}}$ of the fissioning nucleus could be inferred from the measured fragment anisotropy. In terms of this approximate relation, the experimental $\langle J^2 \rangle_{\text{expt}}$ data were deduced with the K_0^2 values of Eq. (1). The ratio $\langle J^2 \rangle_{\text{expt}} / \langle J^2 \rangle_{\text{theory}}$ is shown in Fig. 3 plotted as a function of $E_{\text{c.m.}} / V_B$. Here, the values of $\langle J^2 \rangle_{\text{theory}}$ were extracted from the coupled-channels model [13] fit of the experimental fusion-fission cross sections. The results shown in Fig. 3 again illustrate the effects of the entrance-channel mass asymmetry on fusion-fission processes. For the systems with $\alpha > \alpha_{\text{BG}}$, the data of $\langle J^2 \rangle_{\text{expt}}$ are in agreement with the expectations of the coupled-channels model. However, for the systems with $\alpha < \alpha_{\text{BG}}$, the results of $\langle J^2 \rangle_{\text{expt}}$ are much greater than the theoretical values, $\langle J^2 \rangle_{\text{theory}}$. It should be

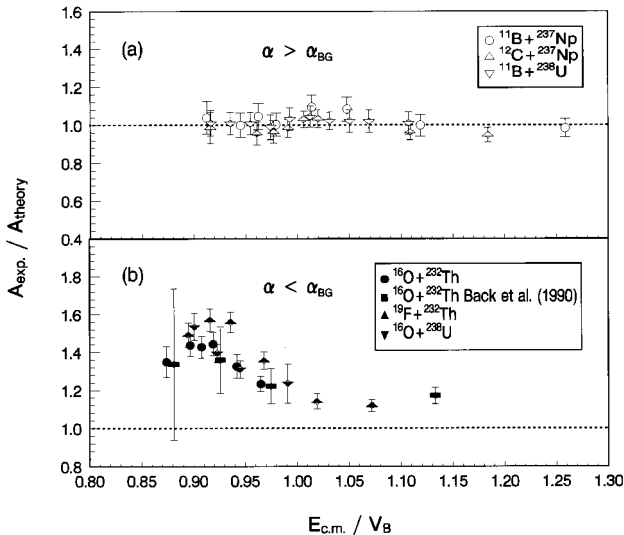


FIG. 2. The ratio of the experimental fragment anisotropy to the value of the SPTS model as a function of $E_{\text{c.m.}} / V_B$ for the systems with $\alpha > \alpha_{\text{BG}}$ (a) and the systems with $\alpha < \alpha_{\text{BG}}$ (b).

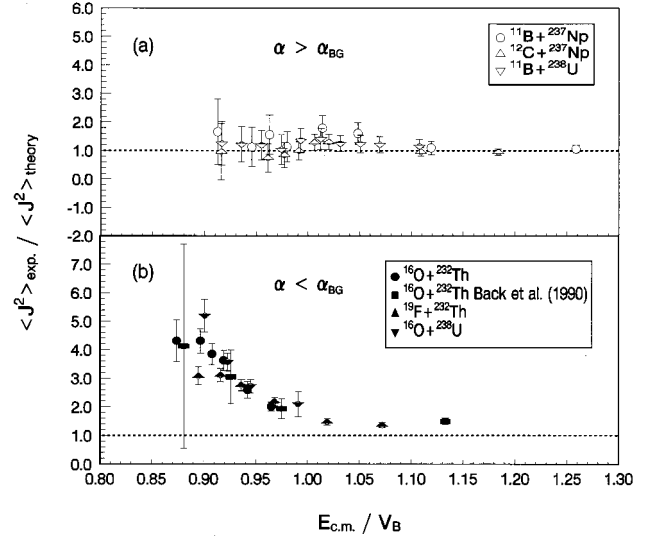


FIG. 3. The ratio, $\langle J^2 \rangle_{\text{expt}} / \langle J^2 \rangle_{\text{theory}}$ as a function of $E_{\text{c.m.}} / V_B$ for the systems with $\alpha > \alpha_{\text{BG}}$ (a) and the systems with $\alpha < \alpha_{\text{BG}}$ (b). Here $\langle J^2 \rangle_{\text{expt}}$ were extracted on the basis of K_0^2 values of Eq. (1).

pointed out here that the data of $\langle J^2 \rangle_{\text{expt}}$ were extracted on the basis of the K_0^2 values. However, we will show later that this basis might not be correct for the fusion-fission reaction systems with the entrance-channel mass asymmetry $\alpha < \alpha_{\text{BG}}$.

IV. DESCRIPTION OF PREEQUILIBRIUM FISSION

Our experimental results apparently illustrate the entrance-channel dependence of fragment anisotropies for a target-projectile combination across the Businaro-Gallone ridge in mass degrees of freedom, therefore provide experimental evidence for preequilibrium fission. In the case of low angular momentum for the systems with $\alpha < \alpha_{\text{BG}}$, the relaxation time of K degrees of freedom may be longer than the fission lifetime. If the relaxation process of K degrees of freedom is taken into account, then the variance of the K distribution, σ_K^2 can be expressed as

$$\sigma_K^2 = K_0^2 \left[1 - \exp\left(-\frac{t}{\tau_K}\right) \right], \quad (4)$$

where τ_K is the relaxation time of K degrees of freedom and K_0^2 is the statistical equilibrium value of σ_K^2 , which is given by Eq. (1). Døssing and Randrup [19] studied the dynamical evolution of angular momentum in damping nuclear reactions, and derived the coupled equations which governed the evolution of the K distribution. They have the expression for the relaxation time of K degrees of freedom which depends on the rotational frequency ω_R . Under some approximations [8], we obtained the following equation for preequilibrium fission:

$$\sigma_K^2(J) = K_0^2 [1 - \exp(-\mathcal{G}J^2)] \quad (5)$$

with $\mathcal{G} = 2.238 \mathcal{G}_{\parallel}^2 / (\mathcal{G}_{\perp}^2 \mathcal{G}_{\text{eff}})$. We did not adjust any parameters in the calculations with this equation.

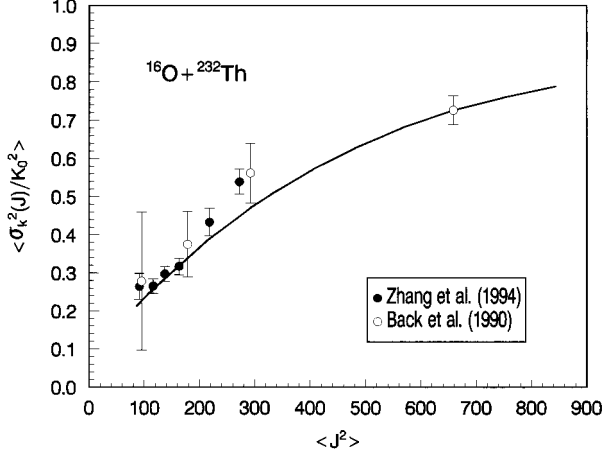


FIG. 4. $\langle \sigma_K^2(J)/K_0^2 \rangle$ vs mean-square angular momentum $\langle J^2 \rangle$ for the reaction system $^{16}\text{O} + ^{232}\text{Th}$.

Figure 4 shows the ratio $\langle \sigma_K^2(J)/K_0^2 \rangle$ versus the mean-square angular momentum $\langle J^2 \rangle$. The solid point and open circles are the results extracted from the measured fragment anisotropies [11,17] of the reaction system $^{16}\text{O} + ^{232}\text{Th}$. The solid curve is the theoretical predictions of the preequilibrium fission model in terms of Eq. (5). The average value of $\sigma_K^2(J)/K_0^2$ is defined as

$$\left\langle \frac{\sigma_K^2}{K_0^2} \right\rangle = \frac{\sum_{J=0}^{\infty} \sigma_F(J) [\sigma_K^2(J)/K_0^2]}{\sum_{J=0}^{\infty} \sigma_F(J)}. \quad (6)$$

It may be seen from Fig. 4 that K degrees of freedom has not reached full equilibration for low angular momentum in the fusion-fission reaction of $^{16}\text{O} + ^{232}\text{Th}$. The agreement between the experimental and theoretical results gives support of the exponential dependence of σ_K^2 on J^2 . As the value of J^2 increases, τ_K decreases rapidly so that K degrees of freedom achieves its equilibrium distribution at saddle point. Therefore, the preequilibrium fission only takes place at low angular momentum. Due to the fact that the contribution of low angular momenta to the total fusion cross section decreases as the bombarding energy increases, the predictions of our preequilibrium fission model gradually tends to coincide with the expectations of the SPTS model as the bombarding energy increasing over V_B . This trend is in agreement with the experimental observations.

To test the availability of our preequilibrium fission model, we have recalculated the theoretical fragment anisotropies in terms of Eq. (5) for the reaction systems with $\alpha < \alpha_{\text{BG}}$, and compared the calculated results with the experimental data in Fig. 5. Also displayed in Fig. 5 are the results of the systems with $\alpha > \alpha_{\text{BG}}$, where the theoretical fragment anisotropies were calculated by the SPTS model. It is evident that the theoretical predictions are in general agreement with the measured results. Therefore, the anomalous fragment anisotropies from the fusion-fission reactions in the near- and subbarrier energy regions are rather successfully explained by means of our preequilibrium fission model. For the reaction systems with $\alpha < \alpha_{\text{BG}}$, we also re-

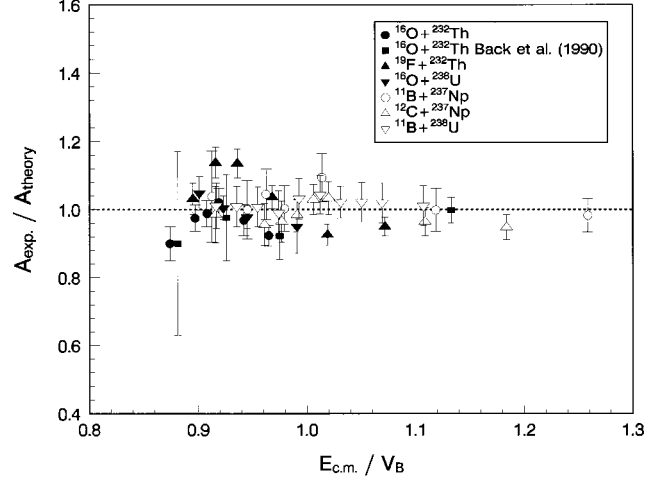


FIG. 5. The ratio $A_{\text{expt}}/A_{\text{theory}}$ as a function of $E_{\text{c.m.}}/V_B$. The values of A_{theory} were calculated in terms of the SPTS model and the preequilibrium fission model for the systems with $\alpha > \alpha_{\text{BG}}$ and $\alpha < \alpha_{\text{BG}}$, respectively.

extracted the mean-square angular momentum $\langle J^2 \rangle_{\text{expt}}$ from the measured fragment anisotropies in terms of the average values of $\sigma_K^2(J)$ defined as

$$\langle \sigma_K^2(J) \rangle = \frac{\sum_{J=0}^{\infty} \sigma_F(J) \sigma_K^2(J)}{\sum_{J=0}^{\infty} \sigma_F(J)}. \quad (7)$$

The results of $\langle J^2 \rangle_{\text{expt}}/\langle J^2 \rangle_{\text{theory}}$ are displayed in Fig. 6. The open symbols are the results of the systems with $\alpha > \alpha_{\text{BG}}$. For these systems, the data of $\langle J^2 \rangle_{\text{expt}}$ were extracted in terms of K_0^2 values of Eq. (1). Figure 7 shows the ratio of the measured fusion-fission cross section to the calculated cross section of the coupled-channels model $\sigma_{\text{expt}}/\sigma_{\text{theory}}$ as a function of $E_{\text{c.m.}}/V_B$ for the reaction systems studied. The results shown in Figs. 6 and 7 lead us to the conclusion that the coupled-channels calculations can give a reasonable self-

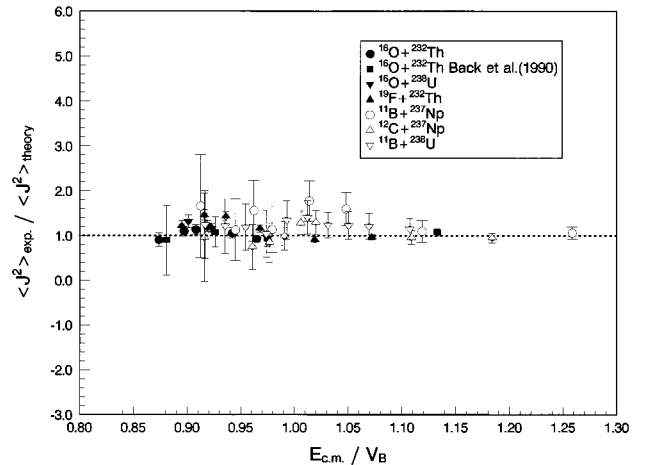


FIG. 6. The ratio $\langle J^2 \rangle_{\text{expt}}/\langle J^2 \rangle_{\text{theory}}$ as a function of $E_{\text{c.m.}}/V_B$. The data $\langle J^2 \rangle_{\text{expt}}$ were extracted from the fragment anisotropies on the basis of the K_0^2 values of Eq. (1) and the $\langle \sigma_K^2(J) \rangle$ values of Eq. (7) for the systems with $\alpha > \alpha_{\text{BG}}$ and $\alpha < \alpha_{\text{BG}}$, respectively.

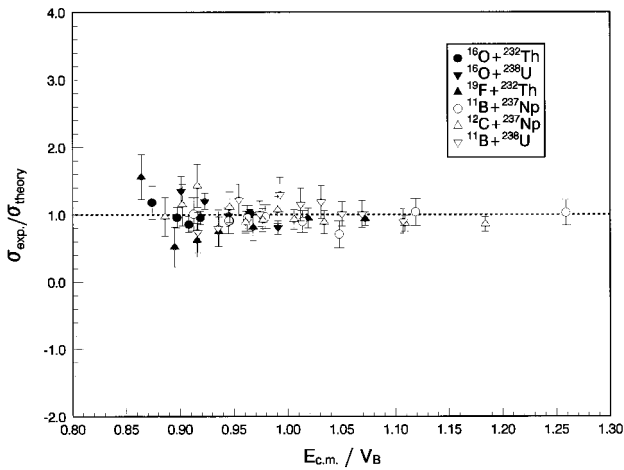


FIG. 7. The ratio of the experimental fusion-fission cross section to the calculated value of the coupled-channels model as a function of $E_{\text{c.m.}}/V_B$.

consistent account of both fusion excitation functions and angular momentum data for fusion-fission reactions.

V. SUMMARY

In the present work, we have demonstrated experimentally that the reaction systems on the different side of the Businaro-Gallone critical mass asymmetry have different

characteristics in fusion-fission reactions. For the systems with $\alpha > \alpha_{\text{BG}}$, the measured fragment anisotropies are in general agreement with the expectation of the SPTS model. However, for the systems with $\alpha < \alpha_{\text{BG}}$, the experimental fragment anisotropies are considerably greater than expectations of the SPTS model at sub-barrier and near-barrier energies and gradually tend to coincide with the theoretical predictions as the bombarding energy increasing over V_B . These observations lead us to the suggestion that the composite systems with their entrance-channel mass asymmetry $\alpha < \alpha_{\text{BG}}$ proceed towards fission with some memories of the entrance-channel plane. It has to be pointed out that the failure for the spherical compound-nucleus formation is the prerequisite for preequilibrium fission. Under this prerequisite, in the case of low angular momentum, the relaxation time of K degrees of freedom will be longer than fission lifetime. By taking the relaxation process of K degrees of freedom into account, we have the expression of $\sigma_K^2(J)$ for preequilibrium fission. In the framework of our preequilibrium fission model, the puzzling problem of the anomalous fragment anisotropies is successfully solved and the discrepancy between the experimental mean-square angular momenta $\langle J^2 \rangle_{\text{expt}}$ and the predictions of the coupled-channels model $\langle J^2 \rangle_{\text{theory}}$ is reasonably removed. Thus, we may conclude that the coupled-channels calculations can give a self-consistent account of both fusion excitation functions and angular momentum data not only for systems leading to nonfissioning nuclei [20,21] but also for systems leading to fissionable nuclei.

-
- [1] L.C. Vaz and J.M. Alexander, *Phys. Rep.* **97**, 1 (1983).
 [2] B.B. Back, *Phys. Rev. C* **31**, 2104 (1985).
 [3] C. Gregoire, C. Ngo, and V. Remand, *Phys. Lett.* **99B**, 17 (1985).
 [4] W.J. Swiatecki, *Phys. Scr.* **24**, 113 (1981).
 [5] R. Vandenbosch, T. Murakami, C.-C. Shahn, D.D. Leach, A. Rag, and M.J. Murphy, *Phys. Rev. Lett.* **56**, 1234 (1986); T. Murakami, C.-C. Shahn, R. Vandenbosch, D.D. Leach, A. Ray, and M.J. Murphy, *Phys. Rev. C* **34**, 1353 (1986).
 [6] H.Q. Zhang, J.C. Xu, Z.H. Liu, J. Lu, K. Xu, and M. Ruan, *Phys. Lett. B* **218**, 133 (1989); H.Q. Zhang, J.C. Xu, Z.H. Liu, M. Ruan, and K. Xu, *Phys. Rev. C* **42**, 1086 (1990).
 [7] D.J. Hinde, M. Dasgupta, J.R. Leigh, J.C. Mein, C.R. Morton, J.O. Newton, and H. Timmers, *Phys. Rev. Lett.* **74**, 1295 (1995).
 [8] Z.H. Liu, H.Q. Zhang, J.C. Xu, Y. Qiao, X. Qian, and C.J. Lin, *Phys. Lett. B* **353**, 173 (1995).
 [9] V.S. Ramamurthy and S.S. Kapoor, in *Proceedings of the International Conference on Nuclear Physics*, Harrogate, United Kingdom, 1986, edited by J.L. Durell, J.M. Irvine, and G.C. Morrison, IOP Conference Proceedings No. 86 (Institute of Physics, Bristol, 1986), Vol. 1, p. 292.
 [10] V.S. Ramamurthy, S.S. Kapoor, R.K. Choudhry, A. Saxena, D.M. Nadkarni, A.K. Mohanty, B.K. Nayak, S.V. Sastry, S. Kailas, A. Chatterjee, P. Singh, and A. Navin, *Phys. Rev. Lett.* **65**, 25 (1990).
 [11] H.Q. Zhang, Z.H. Liu, J.C. Xu, X. Qian, Y. Qiao, C.J. Lin, and K. Xu, *Phys. Rev. C* **49**, 926 (1994).
 [12] H.Q. Zhang, Z.H. Liu, J.C. Xu, X. Qian, S.L. Chen, and L. Lu, *Phys. Rev. C* **47**, 1039 (1993).
 [13] J. Fernandez-Niello, C.H. Dasso, and S. Landowne, *Comput. Phys. Commun.* **54**, 409 (1989).
 [14] A.J. Sierk, *Phys. Rev. C* **33**, 2039 (1986).
 [15] H. Rossner, D.J. Hinde, J.R. Leigh, J.P. Lestone, J.O. Newton, J.X. Wei, and S. Elfstrom, *Phys. Rev. C* **45**, 719 (1992).
 [16] A. Saxena, S. Kailas, A. Karnik, and S.S. Kapoor, *Phys. Rev. C* **47**, 403 (1993).
 [17] B.B. Back, R.R. Betts, P. Fernandez, B.G. Glagole, T. Happ, D. Henderson, H. Ikezoe, and P. Bent (unpublished); and private communication.
 [18] B.B. Back, R.R. Betts, J.E. Gindler, B.D. Wilkins, S. Saini, M.B. Tsang, C.K. Gelbke, W.G. Lurch, M.A. McMahan, and P.A. Baisden, *Phys. Rev. C* **32**, 195 (1985).
 [19] T. Dössing and J. Randrup, *Nucl. Phys.* **A433**, 215 (1985).
 [20] R. Vandenbosch, *Annu. Rev. Nucl. Part. Sci.* **42**, 447 (1992).
 [21] D.E. DiGregorio and R.G. Stokstad, *Phys. Rev. C* **43**, 265 (1991).